2011 American Control Conference
on O'Farrell Street, San Francisco, CA, USA
June 29 - July 01, 2011

A Global Optimization Algorithm for Energy-Efficient Control Allocation of Over-Actuated Systems

Yan Chen and Junmin Wang*
Department of Mechanical and Aerospace Engineering
The Ohio State University
Columbus, OH 43210

Abstract—**This paper presents a new global optimization algorithm for energy-efficient control allocation (CA) scheme, which was proposed for improving operational energy efficiency of over-actuated systems. For a class of realistic power and efficiency functions, a Karush-Kuhn-Tucker (KKT) based algorithm is proposed to find all the local optimal solutions, and consequently the global minimum through a further simple comparison among the entire realistic local minima. This KKT-based algorithm is also independent on the selections of initial conditions by transferring the standard nonlinear optimization problem into classical eigenvalue problems. Numerical examples about practical electric ground vehicles with in-wheel motors are utilized to demonstrate the effectiveness of the proposed global optimization algorithm for the energy-efficient CA problems.**

I. Introduction

OVER-ACTUATED systems, in which the number of actuators is greater than the degrees of freedom, have attracted increasing attention recently [1]-[5]. Many existing physical systems, such as marine vessels [6][7], airplanes [8][9][10], and ground vehicles [11]-[16], can be classified as over-actuated systems because redundant actuators are utilized to improve system performance, reliability and reconfigurablity.

In order to coordinate the redundant actuators and control the over-actuated systems in an elegant configuration, the main challenge is to handle the actuator redundancy and physical constraints simultaneously. Control allocation (CA), as a feasible and promising method, is commonly employed in over-actuated systems to optimally allocate the desired virtual (generalized) control efforts among all the available actuators within their respective constraints, see surveys [6][9] and the references therein. Many different CA algorithms, such as direct allocation [17], daisy-chain allocation [18], (redistributed) pseudo-inverse allocation [14][19], optimization-based allocation [8], and adaptive allocation [20] have been proposed based on different methods to distribute the virtual control.

Although the aforementioned CA methods have different strengths and limitations, numerical optimization-based algorithms are becoming more and more widely used in CA [7][8][13][21]-[23]. Sørdalen [7] adopted the magnitude of actuation as a secondary optimization term in CA formulation in order to achieve minimum control effort. Bodson [8] summarized and evaluated error minimization, control minimization, and mixed error and control optimization problems for optimization-based CA methods. Härkegård [21] suggested a dynamic CA method by penalizing virtual control at previous sampling time in the secondary optimization term. Moreover, Zaccarian [23] described a dynamic CA by inserting a dynamic system as an allocator between the high-level controller and low-level actuators.

Within the aforementioned optimization-based allocation methods, the optimal algorithms to solve various CA problems were similar although the problem formulations were different. Standard numerical algorithms, such as quadratic programming, active-set, and fixed-point, were applied to solve various equivalent nonlinear programming problems of CA. However, local minima were usually obtained by adopting these standard numerical algorithms for general nonlinear programming CA problems. On the other hand, the selections of the initial conditions of these standard algorithms also strongly influence the acquisition of the global minimum. Although there are no uniform optimization algorithms for general nonlinear programming problems, this paper proposes a global and initial-condition-independent algorithm for energy-efficient CA [26] based on Karush-Kuhn-Tucker (KKT) conditions. In the expression of energy-efficient CA problems, a special nonlinear programming is considered since the secondary optimization term, standing for the power consumption of systems, usually consists of polynomial and/or fractional functions. By utilizing this kind of characteristics, the nonlinear programming procedure for energy-efficient CA can be transferred into classical eigenvalue problems, which are initial-condition-independent, based on the KKT conditions. Thus, all the physically meaningful eigenvalues are obtained as local minima of energy-efficient CA problems. Through simple comparisons and exclusions, a global minimum can be obtained.

The remainder of this paper is organized as follows. In section II, both single-mode and dual-mode of the energy-efficient CA schemes are reviewed and briefly described. The KKT condition based algorithm is proposed to find the global minimum for the energy-efficient CA in section III. In section IV, numerical examples based on electric ground vehicle with in-wheel motor dynamics and experimental data are presented to show the effectiveness of the proposed global optimization methods. Conclusive remarks and future work are presented in section V.

*Corresponding author. Authors' emails: chen.1843@osu.edu and wang.1381@osu.edu. This research was supported by the Office of Naval Research (ONR) Young Investigator Award under Grant N00014-09-1-1018, Honda-OSU Partnership Program, and OSU Transportation Research Endowment Program.

II. REVIEW ON ENERGY-EFFICIENT CONTROL ALLOCATION

In this section, the main ideas and formulations of single-mode and dual-mode energy-efficient CA are reviewed for self-completeness. For more details and discussions on energy-efficient CA, the literature [26] is referred.

A. Single-mode energy-efficient CA

A general over-actuated dynamic system is described as follows,

$$\begin{aligned} \dot{x} &= f(x) + g(x)v_d \\ v_d &= Bu \\ y &= h(x) \end{aligned}, \tag{1}$$

where the system state vector is represented by $x \in R^n$, $y \in R^m$ is the system output vector, $v_d \in R^m$ is the virtual control vector, $B \in R^{m\times p}$ is the control effectiveness matrix, and $u \in R^p$ is the system actuator vector. For over-actuated systems, $p > m$ holds as the number of actuators is greater than the number of virtual control signals. Thus, there is no unique solution for u in general and CA is often utilized to address the $R^p \to R^m$ optimal mapping problem.

For over-actuated systems in which each actuator has only one actuation mode and one corresponding efficiency function, the energy-efficient control allocation is formulated as

$$\begin{aligned} &\min\ J = \|W_v(Bu - v_d)\| + \lambda P_c, \\ &\text{s.t. } u_{min} \le u \le u_{max}, \end{aligned} \tag{2}$$

where P_c is the total instantaneous power consumption by all the actuators. A small positive parameter λ is used to balance the efforts between reducing CA errors and the power consumptions. The power consumption could be a function of actuation forces or torques based on the corresponding actuator efficiency functions, which can be expanded as follows,

$$P_c = \sum_{i=1}^{p} P_{ci}(u_i) = \sum_{i=1}^{p} \frac{P_{oi}(u_i)}{\eta_{oi}(u_i)}. \tag{3}$$

Within equation (3), $P_{oi}(u_i)$ and $\eta_{oi}(u_i)$ are the output power function and the efficiency function of the i^{th} actuator, respectively. Therefore, the division between $P_{oi}(u_i)$ and $\eta_{oi}(u_i)$ represents the i^{th} actuator's power consumption P_{ci}. Thus, the formulation of single-mode energy-efficient CA is built in (2) and (3).

B. Dual-mode energy-efficient CA

When actuators in physical systems have dual working modes, such as consuming and gaining energy, and different associated efficiency functions/characteristics, the expression of the over-actuated dynamic systems described in (1) is correspondingly augmented as,

$$\begin{aligned} \dot{x} &= f(x) + g(x)v_d \\ v_d &= B_a[u^T \quad u'^T]^T. \\ y &= h(x) \end{aligned} \tag{4}$$

A virtual actuator vector $u' \in R^q,\ 1 \le q \le p$ is introduced to represent the q dual-mode actuators involved in the system. The augmented matrix $B_a = [B \quad B_q] \in R^{m\times(p+q)}$ is the new control effectiveness matrix for the new nonlinear system.

The energy-efficient CA scheme (2) and (3) is modified for the new augmented system (4) with dual-mode actuators as

$$\begin{aligned} &\min\ J = \|W_v(B_a[u^T \quad u'^T]^T - v_d)\| + \lambda P_c, \\ &\text{s.t. } \begin{cases} u_{min} \le u \le u_{max} \\ u'_{min} \le u' \le u'_{max} \\ u_i u'_i = 0,\ i = 1, \dots, q \end{cases}. \end{aligned} \tag{5}$$

Since a particular dual-mode actuator can only operate in one of the two operating modes at any given time instant, the added third term in the constraints ascertains that only one operating mode is assigned to a physical actuator by the CA. A physical example of dual-model actuator is electric motor which can work on both motor mode (consuming energy from the system) and generator mode (gaining energy to the system).

Within equation (5), the total power consumption P_c thus can include the instantaneous power consumption and gain with respect to the dual operating modes for each of the physical actuators. For example, if u denotes the actuator energy consuming mode and u' represents the actuator energy gaining mode, then the total power consumption of all the actuators in different modes is formulated as

$$P_c = \sum_{i=1}^{p} \frac{P_{oi}(u_i)}{\eta_{oi}(u_i)} - \sum_{i=1}^{q} P_{ii}(u'_i)\eta_{ii}(u'_i). \tag{6}$$

Within equation (6), P_{oi} and η_{oi} denote the actuator output power and efficiency at the energy consuming mode. While P_{ii} and η_{ii} represent the actuator input power and efficiency at the energy gaining mode, respectively. The energy gaining mode is inferred by the minus sign in front of virtual actuator power consumption. Therefore, the formulation of the dual-mode energy-efficient CA is built in (5) and (6).

III. KKT-BASED GLOBAL OPTIMIZATION ALGORITHMS FOR ENERGY-EFFICIENT CONTROL ALLOCATION

For both single-mode and dual-mode energy-efficient CA, the authors adopted a standard nonlinear optimization method, active-set algorithm, to obtain the solutions [26]. The adopted algorithm, however, cannot guarantee the global optimization and are sensitive to the selections of initial conditions. Based on the KKT conditions, a global and initial-condition-independent optimization algorithm is proposed for energy-efficient CA in the following section.

A. KKT conditions for the single-mode energy-efficient CA

In order to develop the optimization algorithm for the single-mode energy-efficient CA, the expressions (2) and (3) are combined and modified as

$$\begin{aligned} &\min\ J = \|W_v(Bu - v_d)\|^2 + \lambda P_o^T(u)\frac{1}{\eta_o(u)}, \\ &\text{s.t. } \begin{cases} u - u_{min} \ge 0 \\ u_{max} - u \ge 0 \end{cases}. \end{aligned} \tag{7}$$

The square modification for CA errors is good for derivatives of the Lagrangian function defined in the following. $P_o(u), \eta_o(u) \in R^p$ are the vector forms of output power functions and efficiencies, respectively.

Define the following Lagrangian function

$$L(u, \underline{\lambda}, \overline{\lambda}) = J(u, \lambda) - \underline{\lambda}^T(u - u_{min}) - \overline{\lambda}^T(u_{max} - u). \tag{8}$$

Within (8), nonnegative vectors $\underline{\lambda}$ and $\overline{\lambda} \in R^p$ are Lagrangian multipliers. Based on the KKT conditions [27], the optimal solution u^* with certain Lagrangian multipliers $\underline{\lambda}^*$ and $\overline{\lambda}^*$ satisfy the following conditions:

$$\frac{\partial L(u,\overline{\lambda},\underline{\lambda})}{\partial u}\Big|_{\substack{u=u^* \\ \underline{\lambda}=\underline{\lambda}^* \\ \overline{\lambda}=\overline{\lambda}^*}} = 2B^T W_v^T W_v (Bu^* - v_d) + \lambda \frac{\dot{P}_o^T(u^*)\eta_o(u^*) - P_o^T(u^*)\dot{\eta}_o(u^*)}{\eta_o^2(u^*)} - \underline{\lambda}^* + \overline{\lambda}^* = 0 \quad (9)$$

$$(\underline{\lambda}_i^*)(u^* - u_{min})_i = 0,\ (\overline{\lambda}_i^*)(u_{max} - u^*)_i = 0,$$

$$u^* - u_{min} \geq 0\ ,\ u_{max} - u^* \geq 0, \overline{\lambda}^* \geq 0,\ \underline{\lambda}^* \geq 0.$$

Generally, the KKT conditions can characterize the global optimal solution when the objective/cost function and the constraint set are convex. Although the cost function in (7) is not in a convex form, further examinations can be fulfilled to exclude the maximum and the local minima. For the special form of energy-efficient CA, the corresponding KKT conditions (9) are simple to be checked for obtaining the global minimum.

B. KKT conditions for the dual-mode energy-efficient CA

Similar to the single-mode case, the expressions (5) and (6) are combined and modified so as to develop the optimization algorithm for the dual-mode energy-efficient CA.

$$\min J = \|W_v(B_a[u^T \quad u'^T]^T - v_d)\|^2 + \lambda\left(P_o^T(u)\frac{1}{\eta_o(u)} - P_i^T(u')\eta_i(u')\right), \quad (10)$$

$$\text{s.t.} \begin{cases} u - u_{min} \geq 0 \\ u_{max} - u \geq 0 \\ u' - u'_{min} \geq 0, \\ u'_{max} - u' \geq 0 \\ u_i u'_i = 0 \end{cases}$$

where $P_i(u'), \eta_i(u') \in R^q$ are the vector forms of input power functions and efficiencies, respectively.

Define the corresponding Lagrangian function as

$$L(u,u',\overline{\lambda},\underline{\lambda},\overline{\lambda'},\underline{\lambda'}) = J(u,u') - \underline{\lambda}^T(u - u_{min}) - \overline{\lambda}^T(u_{max} - u) - \underline{\lambda'}^T(u' - u'_{min}) - \overline{\lambda'}^T(u'_{max} - u'). \quad (11)$$

Within (11), nonnegative vectors $\overline{\lambda}$ and $\underline{\lambda} \in R^p$, $\overline{\lambda'}$ and $\underline{\lambda'} \in R^q$, are Lagrangian multipliers. Based on the KKT conditions [27], the optimal solutions u^* and u'^* with certain Lagrangian multipliers $\overline{\lambda}^*$, $\underline{\lambda}^*$, $\overline{\lambda'}^*$ and $\underline{\lambda'}^*$ satisfy the following conditions:

$$\frac{\partial L(u,u',\overline{\lambda},\underline{\lambda},\overline{\lambda'},\underline{\lambda'})}{\partial u}\Big|_{\substack{u=u^*,\ \underline{\lambda}=\underline{\lambda}^*,\ \overline{\lambda}=\overline{\lambda}^* \\ u'=u'^*,\ \underline{\lambda'}=\underline{\lambda'}^*,\ \overline{\lambda'}=\overline{\lambda'}^*}} = 2B^T W_v^T W_v (B_a[u^{*T} \quad u'^{*T}]^T - v_d) + \lambda \frac{\dot{P}_o^T(u^*)\eta_o(u^*) - P_o^T(u^*)\dot{\eta}_o(u^*)}{\eta_o^2(u^*)} - \underline{\lambda}^* + \overline{\lambda}^* = 0,$$

$$\frac{\partial L(u,u',\overline{\lambda},\underline{\lambda},\overline{\lambda'},\underline{\lambda'})}{\partial u'}\Big|_{\substack{u=u^*,\ \underline{\lambda}=\underline{\lambda}^*,\ \overline{\lambda}=\overline{\lambda}^* \\ u'=u'^*,\ \underline{\lambda'}=\underline{\lambda'}^*,\ \overline{\lambda'}=\overline{\lambda'}^*}} = 2B_q^T W_v^T W_v (B_a[u^{*T} \quad u'^{*T}]^T - v_d) - \lambda\left[\dot{P}_i^T(u'^*)\eta_i(u'^*) + P_i^T(u'^*)\dot{\eta}_i(u'^*)\right] - \underline{\lambda'}^* + \overline{\lambda'}^* = 0, \quad (12)$$

$$u_i u'_i = 0,$$

$$(\underline{\lambda}_i^*)(u^* - u_{min})_i = 0,\ (\overline{\lambda}_i^*)(u_{max} - u^*)_i = 0,$$

$$(\underline{\lambda'}_i^*)(u'^* - u'_{min})_i = 0,\ (\overline{\lambda'}_i^*)(u'_{max} - u'^*)_i = 0,$$

$$u^* - u_{min} \geq 0\ ,\ u_{max} - u^* \geq 0, u'^* - u'_{min} \geq 0\ ,$$

$$u'_{max} - u'^* \geq 0,\ \overline{\lambda}^* \geq 0,\ \underline{\lambda}^* \geq 0, \overline{\lambda'}^* \geq 0,\ \underline{\lambda'}^* \geq 0,$$

Again, although the KKT conditions, in general, cannot guarantee the global optimal solution of the non-convex cost function (10), further examinations can be fulfilled to exclude the maximum and the local minima. For the special form of energy-efficient CA, the corresponding KKT conditions (12) are simple to be checked for obtaining the global minimum.

IV. NUMERICAL EXAMPLES AND DISCUSSIONS

In this section, the aforementioned KKT conditions for both single-mode and dual-mode energy-efficient CA are applied to numerical examples. These examples are abstracted from practical electric ground vehicle in-wheel/hub motor models and experimental data [28], from which the assumption and validation of the aforementioned formulation are verified.

In-wheel motor technology has become mature and allows fast and accurate torque control for each of the electric ground vehicle (EGV) wheels. Electric concept cars with independently actuated in-wheel motors such as the GM Geo Storm and Volvo ReCharge have already proceeded into the prototyping and/or pre-market phases. Thus, in-wheel/hub motors have strongly potential applications in automotive industry, see [13][26] and references therein. Compared with the conventional vehicle drivetrain architectures where driving and braking actions of different wheels are coupled, EGVs with independently actuated in-wheel motors can offer higher control flexibility and many potential advantages [29]. Consequently, the efficiency and control allocation problem are meaningful to be investigated.

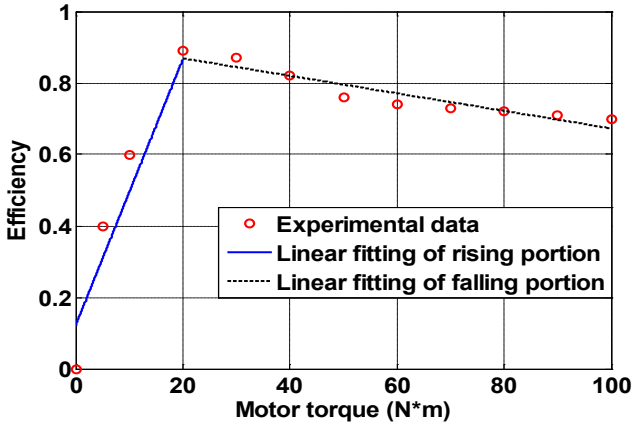

Figure 1. The efficiency curve fitting of an in-wheel BLDC motor and its controller based on experimental data.

The output efficiency function $\eta_o(u)$ of an in-wheel BLDC motor and its controller is expressed by fitting the experimental data shown in Figure 1. Two linear functions are adopted to approximate the rising and falling portions of the entire experimentally measured data.

$$\eta_o(u) = \begin{cases} a_{11}u + b_{11}, & 0 \le u < 20, \\ a_{12}u + b_{12}, & 20 \le u \le 100, \end{cases} \quad (13)$$

where a_{11}, b_{11}, a_{12} and b_{12} are coefficients, listed in Table 1.

Table 1 Efficiency Function Parameters

Symbol	Values
a_{11}	0.0372
b_{11}	0.122
a_{12}	-0.0025
b_{12}	0.9181

Multiple reasons make the piece-wise linear function (13) as the efficiency fitting function. The first one is the consideration of computational effort. From either (9) or (12), the KKT conditions offer algebra equations or eigenvalue problems to obtain the optimal values. The simpler efficiency fitting function makes the computational cost less. The second reason is due to the DC characteristics of the BLDC motors. The piece-wise linear function (13) can sufficiently describe the rising and falling trend along with the increase of motor torque. Last but not the least, although the motor speed also slightly affects the motor efficiency as can be seen from Figure 2, the efficiency curves are similar within a large range of rotational speeds [28]. Moreover, motor rotational speed can be reasonably assumed to be a constant at each instantaneous time for CA due to the short sampling period.

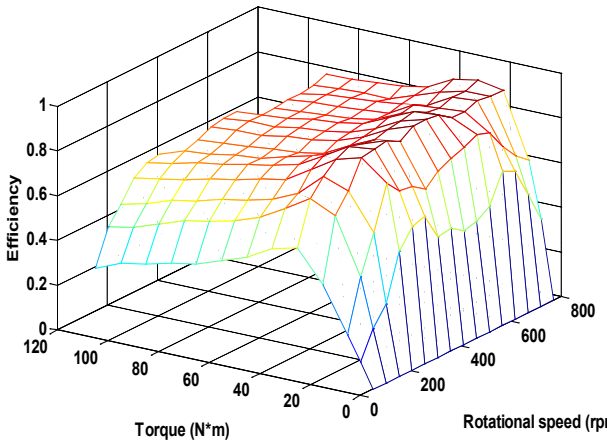

Figure 2. The driving efficiency map of an in-wheel BLDC motor based on experimental data.

The power consumption of the in-wheel motor is given by

$$P_o(u) = u\omega_0, \quad (14)$$

where ω_0 is a given rotational speed and u stands for the motor torque. Without loss of generality, two in-wheel BLDC motors are considered for the longitudinal speed control of a bicycle vehicle model under straight line driving conditions. Different scaling ratios are applied to the efficiency curve in Figure 1 to generate different efficiency functions for two motors and two working modes. In the case of single-mode actuation (both in-wheel motors drive), the control effectiveness matrix $B = [1\ 1]^T$. In the case of dual-mode actuation (both in-wheel motors can drive and regenerative brake), the control effectiveness matrix $B_a = [1\ 1\ 1\ 1]^T$. The boundary of the actuator are $u_{min} = 0$ and $u_{max} = 100$ for driving and $u'_{min} = -100$ and $u'_{max} = 0$ for regenerative braking.

A. Single-mode energy-efficient CA

In the numerical example for single-mode energy-efficient CA, the rotational speed $\omega_0 = 400$ rpm, which is about 50 km/h for a passage car with common tire effective radius around 0.3 meter. The penalty coefficient λ is set to be 0.001 and the weighting matrix W_v was set to be an identity matrix for the optimization problem. The scaling ratio for efficiency of the second in-wheel motor was 0.9.

Substituting (14) into (9) and letting $\underline{\lambda}^* = \overline{\lambda}^* = 0$ for nontrivial solutions, the following equations are obtained,

$$\begin{aligned} 2(u_1^* + u_2^* - v_d) + \lambda \frac{\dot{P}_{o1}(u_1^*)\eta_{o1}(u_1^*) - P_{o1}(u_1^*)\dot{\eta}_{o1}(u_1^*)}{\eta_{o1}^2(u_1^*)} = 0, \\ 2(u_1^* + u_2^* - v_d) + \lambda \frac{\dot{P}_{o2}(u_2^*)\eta_{o2}(u_2^*) - P_{o2}(u_2^*)\dot{\eta}_{o2}(u_2^*)}{\eta_{o2}^2(u_2^*)} = 0. \end{aligned} \quad (15)$$

Since the efficiency function (13) is piece-wise linear, the equations (15) have to be solved by combining different efficiency functions. Basically, four pairs of two algebraic equations are obtained. In order to solve two algebraic equations with two variables, like (15), classical eigenvalue problems can be formulated. Thus, the optimization problem are transferred into multiple eigenvalue problems to find the optimal u_1^* and u_2^*. Compared with the trivial solutions (boundary values of actuators), the global optima can be finally obtained. Given different virtual control v_d, the following CA results without considering choice of initial values are obtained.

Table 2 Single-mode energy efficient CA results

v_d (N*m)	u_1^* (N*m)	u_2^* (N*m)	P_{ce} (Watt)	P_{cs} (Watt)
10	10	0	847.9	1436
20	20	0	967.4	1790
40	20	20	2040	2040
60	38.87	21.11	3120	3147
80	48.61	31.37	4296	4324

In Table 2, the symbol P_{ce} stands for the instantaneous power consumption by using energy-efficient CA and the symbol P_{cs} represents the instantaneous power consumption by using a standard CA method, which has an equal torque distribution on two in-wheel motors. From the values in the 4th and 5th columns, the energy-efficient CA algorithm indeed costs less power than the standard CA method. It is interesting to observe the case of $v_d = 40$. The power consumptions of two allocation methods are the same because the average torque distribution happens to be the most energy efficient one, which can be seen from Figure 1 and the efficiency scaling assumption.

Moreover, when the virtual control v_d is small, the energy-efficient CA algorithm automatically determines only the first in-wheel motor is used because of a higher efficiency. Along with the increase of the virtual control, the first

in-wheel motor cannot guarantee to be working alone in a high-efficiency regime. Thus, a part of the virtual torque is distributed to the second in-wheel motor to make both motors work in high-efficiency regimes, consequently to optimize the total consumed power. The CA results listed in Table 2 are obtained without giving any initial values of u_1 and u_2 by solving the equivalent eigenvalue problem. The global optimization of the distribution torques u_1^* and u_2^* are verified from the following plot in Figure 3.

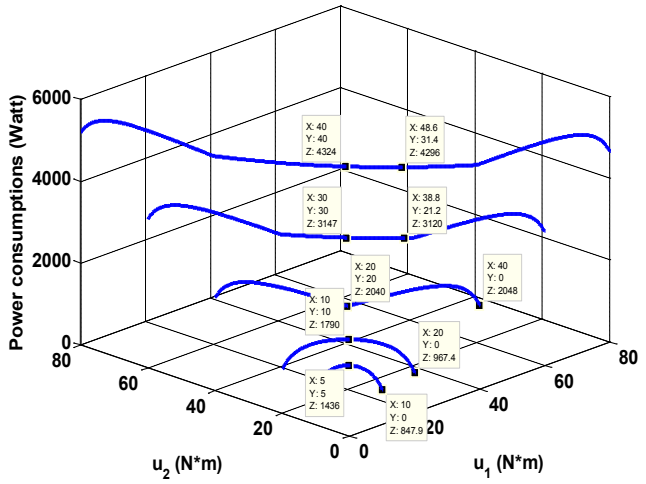

Figure 3. Power consumption of single-mode energy-efficient CA with two actuators.

Figure 3 shows the cost function of optimization problem (2) and (3) by inserting efficiency and power expressions (13) and (14) in. Each curve in Figure 3 represents different virtual control from 10 to 80, the same as those in Table 2. On each curve, the corresponding virtual control is equal to the sum of distributions on two motors. Except the case of $v_d = 40$, all the labels on the left side show the distribution results of the standard CA and all the labels on the right in Figure 3 represent the global optimization points. Although these global minimum points vary on the non-convex curves, the proposed KKT-based algorithm accurately finds all of them from the equivalent eigenvalue problems. If a standard active-set algorithm is applied to solve the nonlinear optimization problem, the global minimum points may not be found by inappropriate choices of initial conditions and only local minima are obtained.

B. Dual-mode energy-efficient CA

The same values for rotational speed ω_0, weighting matrix W_v, and the penalty coefficient λ as those in the single-mode case were adopted for the numerical example in dual-mode energy-efficient CA. Assuming that two in-wheel motors (front and rear) with the same type (such as BLDC) have the similar efficiency profile, the scaling ratio for the driving efficiency of the rear motor is 0.9. Moreover, the regenerative braking efficiency is usually less than the driving efficiency. Thus, the scaling ratio for the regenerative braking efficiency of each motor is set as 0.9 of the corresponding driving efficiency.

Substituting (14) into (12) and letting $\underline{\lambda}^* = \overline{\lambda}^* = \overline{\lambda'}^* = \underline{\lambda'}^* = 0$ for nontrivial solutions, the following expressions are obtained,

$$
\begin{aligned}
&2(B_a u^* - v_d) + \lambda \frac{\dot{P}_{o1}(u_1^*)\eta_{o1}(u_1^*) - P_{o1}(u_1^*)\dot{\eta}_{o1}(u_1^*)}{\eta_{o1}^2(u_1^*)} = 0,\\
&2(B_a u^* - v_d) + \lambda \frac{\dot{P}_{o2}(u_2^*)\eta_{o2}(u_2^*) - P_{o2}(u_2^*)\dot{\eta}_{o2}(u_2^*)}{\eta_{o2}^2(u_2^*)} = 0,\\
&2(B_a u^* - v_d) -\\
&\lambda\left(\dot{P}_{i1}(u_1'^*)\eta_{i1}(u_1'^*) + P_{i1}(u_1'^*)\dot{\eta}_{i1}(u_1'^*)\right) = 0,\\
&2(B_a u^* - v_d) -\\
&\lambda\left(\dot{P}_{i2}(u_2'^*)\eta_{i2}(u_2'^*) + P_{i2}(u_2'^*)\dot{\eta}_{i2}(u_2'^*)\right) = 0,\\
&u_1^* u_1'^* = 0,\ u_2^* u_2'^* = 0.
\end{aligned}
\tag{16}
$$

Like the process in the single-mode case, similar steps were implemented to solve (16) by plugging in the piece-wise linear efficiency function (13). Then, comparison with trivial solutions will give the global optimal solutions. Given different virtual control v_d, the following CA results without considering choices of initial values are obtained.

Table 3 Dual-mode energy efficient CA results

v_d (N*m)	u_1^* (N*m)	u_2^* (N*m)	$u_1'^*$ (N*m)	$u_2'^*$ (N*m)	P_{ce} (Watt)
4	20	0	0	-16	575.7
8	20	0	0	-12	733.6
10	20	0	0	-10	797.4
20	20	0	0	0	967.4

In Table 3, the symbol P_{ce} stands for the instantaneous power consumption by using energy-efficient CA. From the values in the 2nd and 5th columns, the energy-efficient CA algorithm distributes torques to the driving mode of the front motor and the regenerative braking mode of the rear motor when the virtual control is small. Since if only the front motor is actuated, the efficiency is very low for small v_d. By exciting the regenerative braking mode of the rear motor, not only the rear motor gains energy at a relative high-efficiency rate, but the front motor also works at a higher efficiency point to consume less power. Thus, the total consumption power is less than the single motor actuation case. It is interesting to observe the case of $v_d = 10$. The power consumption of the dual-mode algorithm is less than that of the single-mode case for the same virtual control, which displays the necessity and advantage of the dual-mode energy-efficient CA algorithm.

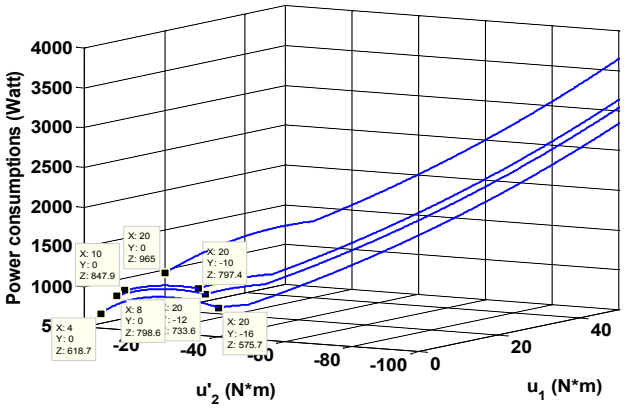

Figure 4. Power consumption of dual-mode energy-efficient CA with two actuators.

Along with the increase of the virtual control, only the most efficient mode in the first motor is excited because the

equivalent efficiency of the regenerative braking and driving case is lower than the single-motor driving case, which can be seen from the 5th row in Table 3. By further increasing the virtual control, the dual-mode energy-efficient CA enters the single-mode distribution algorithm. The CA results listed in Table 3 are obtained without giving any initial values by solving the equivalent eigenvalue problem. The global optimization of the distribution torques u_1^*, u_2^*, $u_1'^*$ and $u_2'^*$ are verified from the plot in Figure 4.

Figure 4 shows the cost function of optimization problem (5) and (6) by inserting efficiency and power expressions (13) and (14) in. Each curve in Figure 4 represents different virtual control from 4 to 20, the same as those in Table 3. On each curve, the corresponding virtual control is equal to the sum of distributions on the two motors. All the labels on the right in Figure 4 represent the global optimization points. Although these global minimum points vary on the non-convex curves, the proposed KKT-based algorithm accurately finds all of them from the equivalent eigenvalue problem. If a standard active-set algorithm is applied to solve the nonlinear optimization problem, the global minimum points may not be found by inappropriate choices of initial conditions and only local minima are obtained.

Moreover, Figure 4 only gives the power consumption under the actuation that the first motor drives and the second motor brakes because the other working pair, the first motor braking and the second motor driving, consumes more power due to the lower driving efficiency of the second motor.

V. Conclusions and Future Work

This paper introduces a new global optimization method for energy-efficient control allocation (CA). By considering the specific nonlinear formulation of the cost function, a KKT-based algorithm is proposed to find the global optimal solution of the energy-efficient CA problem. This KKT-based algorithm does not rely on the choices of initial conditions. Numerical examples about electric ground vehicles with in-wheel motors exhibited the effectiveness of the proposed global optimization energy-efficient CA algorithm.

The real-time implementation of this algorithm will be improved and tested in a platform of electric ground vehicles.

References

[1] M. Benosman, F. Liao, K. Lum and J. L. Wang, "Nonlinear control allocation for non-minimum phase systems," *IEEE Transactions on Control Systems Technology*, Vol. 17, No.2, pp. 394-404, March, 2009.

[2] V. L. Poonamallee, S. Yurkovich, A. Serrani, D. B. Doman and M. W. Oppenheimer, "A nonlinear programming approach for control allocation," *Proceedings of the 2004 American Control Conference*, pp. 1689-1694, 2004.

[3] H. Alwi and C. Edwards, "Fault tolerant control using sliding modes with on-line control allocation," *Automatica*, 44, pp. 1859-1866, 2008.

[4] F. Liao, K. Lum, J. L. Wang and M. Benosman, "Adaptive nonlinear control allocation of non-minimum phase uncertain systems," *Proceedings of the 2009 American Control Conference*, pp. 2587-2592, 2009.

[5] J. Zheng, W. Su and M. Fu, "Dual-stage actuator control design using a doubly coprime factorization approach," *IEEE/ASME Transactions on Mechatronics*, Vol. 15, No. 1, 2010.

[6] T. Fossen and T. Johansen, "A survey of control allocation methods for ships and underwater vehicles," *14th Mediterranean conference on control and automation*, 2006.

[7] O. J. Sørdalen, "Optimal thrust allocation for marine vessels," *Control Engineering Practice*, Vol. 5, No. 9, pp. 1223-1231, 1997.

[8] M. Bodson, "Evaluation of optimization methods for control allocation," *Journal of Guidance, Control, and Dynamics*, Vol. 25, No.4, pp. 703-711, 2002.

[9] M. Oppenheimer, D. Doman and M. Bolender, "Control allocation for over-actuated systems," *14th Mediterranean conference on control and automation*, 2006.

[10] D. B. Doman, B. J. Gamble and A. D. Ngo, "Quantized control allocation of reaction control jets and aerodynamic control surfaces," *Journal of Guidance, Control, and Dynamics*, Vol. 32, No.1, pp. 13-24, 2009.

[11] M. Gerard and M. Verhaegen, "Global and local chassis control based on load sensing," *Proceedings of the 2009 American Control Conference*, pp. 677-682, June, 2009.

[12] J. H. Plumlee, D. M. Bevly and A. S. Hodel, "Control of a ground vehicle using quadratic programming based control allocation techniques," *Proceedings of the 2004 American Control Conference*, pp. 4704-4709, Boston, 2004.

[13] J. Wang and R. G. Longoria, "Coordinated and reconfigurable vehicle dynamics control," *IEEE Transactions on Control Systems Technology*, vol. 17, No. 3, pp. 723 – 732, May 2009 (DOI: 10.1109/TCST.2008.2002264).

[14] J. Wang and R. G. Longoria, "Coordinated vehicle dynamics control with control distribution," *Proceedings of the 2006 American Control Conference*, pp. 5348-5353, 2006.

[15] J. Wang, J. M. Solis and R. G. Longoria, "On the control allocation for coordinated ground vehicle dynamics control systems," *Proceedings of the 2007 American Control Conference*, pp. 5724-5729, July, 2007.

[16] J. Wang and R. G. Longoria, "Combined tire slip and slip angle tracking control for advanced vehicle dynamics control systems," *Proceedings of the 45th IEEE Conference on Decision and Control*, pp.1733 – 1738, 2006.

[17] W. C. Durham, "Constrained control allocation," *Journal of Guidance, Control, and Dynamics*, Vol. 16, No.4, pp. 717-725, 1993.

[18] J. M. Buffington and D. F. Enns, "Lyapunov stability analysis of daisy chain control allocation," *Journal of Guidance, Control, and Dynamics*, Vol. 19, No.6, pp. 1226-1230, 1996.

[19] J. Virnig and D. Bodden, "Multivariable control allocation and control law conditioning when control effectors limit," *AIAA paper 94-3609*, 1994.

[20] J. Tjønnås and T. A. Johansen, "Adaptive control allocation," *Automatica*, Vol. 44, pp. 2754-2765, 2008.

[21] O. Härkegård, "Dynamic control allocation using constrained quadratic programming," *Journal of Guidance, Control, and Dynamics*, Vol. 27, No. 6, pp. 1028-1034, 2004.

[22] O. Härkegård, and S. Glad, "Resolving actuator redundancy - optimal control vs control allocation," *Automatica*, Vol. 41, No. 1, pp. 137-144, 2005

[23] L. Zaccarian, "Dynamic allocation for input redundant control systems," *Automatica*, Vol. 45, pp. 1431-1438, 2009.

[24] D. B. Doman and M. W. Oppenheimer, "Improving control allocation accuracy for nonlinear aircraft dynamics," *Proceedings of AIAA Guidance, Navigation, and Control Conference and Exhibit*, pp. 1-10, 2002.

[25] X. Wei, L. Guzzella, V. I. Utkin and G. Rizzoni, " Model-based fuel optimal control of hybrid electric vehicle using variable structure control systems," *Journal of Dynamic Systems, Measurement, and Control,* Vol. 129, No. 1, pp. 13-19, 2007.

[26] Y. Chen and J. Wang, "Energy-efficient control allocation for over-actuated systems with electric vehicle applications," *Proceedings of the 2010 ASME Dynamic Systems and Control Conference*, Boston, 2010.

[27] J. Nocedal and S. Wright, "Numerical Optimization," Springer, 2006.

[28] R. Wang, Y. Chen, D. Feng, X. Huang, and J. Wang, "Development and Performance Characterization of an Electric Ground Vehicle with Independently Actuated In Wheel Motors," *Journal of Power Sources*, Vol. 196, No 8, pp. 3962-3971, 2011.

[29] Yan Chen and Junmin Wang, "Adaptive Vehicle Speed Control with Input Injections for Longitudinal Motion Independent Road Frictional Condition Estimation," *IEEE Transactions on Vehicular Technology*, Vol. 60, No. 3, pp. 839 - 848, 2011.